Biosensors and Bioelectronics 86 (2016) 293–300

Contents lists available at ScienceDirect

Biosensors and Bioelectronics

journal homepage: www.elsevier.com/locate/bios

Highly sensitive sandwich-type SPR based detection of whole H5Nx viruses using a pair of aptamers

Van-Thuan Nguyen [a], Ho Bin Seo [a], Byoung Chan Kim [b], Sang Kyung Kim [c], Chang-Seon Song [d], Man Bock Gu [a,*]

[a] Department of Biotechnology, College of Life Sciences and Biotechnology, Korea University, Anam-dong, Seongbuk-gu, Seoul 136-713, Republic of Korea
[b] Center for Environment, Health and Welfare Research, Korea Institute of Science and Technology (KIST), Department of Energy and Environmental Engineering, Korea University of Science and Technology (UST), Hwarangno 14-gil 5, Seongbuk-gu, Seoul 136-791, Republic of Korea
[c] Center of BioMicrosystems,Korea Institute of Science and Technology (KIST), Hwarangno 14-gil 5, Seongbuk-gu, Seoul 136-791, Republic of Korea
[d] Department of Infectious Diseases, College of Veterinary Medicine, Konkuk University, Kwangjin-gu, Seoul 143-701, Republic of Korea

ARTICLE INFO

Article history:
Received 20 April 2016
Received in revised form
10 June 2016
Accepted 21 June 2016
Available online 21 June 2016

Keywords:
Whole virus H5Nx
Dual aptamer
SPR
AuNP
Circular Dichroism

ABSTRACT

In this research, we report highly sensitive and specific sandwich-type SPR-based biosensor for the detection H5Nx whole viruses. A few of aptamers, for the first time, were successfully screened and characterized for whole avian influenza (AI) viruses, H5Nx, by using Multi-GO-SELEX method. The affinities of the aptamers developed in this study were ranged from 8×10^4 to 1×10^4 EID50/ml, and the aptamers IF22, IF23 were found to be specific to H5N1 and H5N8, respectively. In addition, some flexible aptamers IF20, IF15, and IF10 were found to bind to the H5N1 and H5N2, H5N1 and H5N8, or H5N1, H5N2, and H5N8, respectively. Moreover, aptamers IF10 and IF22 were found to bind H5N1 virus simultaneously and confirmed to bind the different site of the same H5N1 whole virus. Therefore, this pair of aptamers, IF10 and IF22, were successfully applied to develop the sandwich-type SPR-based biosensor assay which is rapid, accurate for the detection of AI whole virus from H5N1-infected feces samples. The minimum detectible concentration of H5N1 whole virus was found to be 200 EID50/ml with this sandwich-type detection using the aptamer pair obtained in this study. In addition, the sensitivity of this biosensor was successfully enhanced by using the signal amplification with the secondary aptamer conjugated with gold nanoparticles.

1. Introduction

Highly pathogenic disease caused by avian influenza A H5Nx viruses, threat to the poultry industry and human worldwide seriously. The highly pathogenic avian influenza (AI) strain H5Nx emerged in Southern China in the 1990 s and the first large-scale epizootic took place in the winter of 2004 in the East and Southeast Asia. The virus persisted in the region until the winter in August 2006–2007 and it was spread over 60 countries (Li, et al. 2004; Alexander, et al. 2007). In addition, all of the previous outbreaks have been costly and difficult to be controlled in the agricultural sector. For highly pathogenic disease, the most important control measures are rapid culling of all infected or exposed birds, proper disposal of carcasses, the quarantining and rigorous disinfection of farms, and the implementation of strict sanitary, or “biodefense”, measures. Restrictions on the movement of live poultry, both within and between countries, are another important control measures.

Highly pathogenic viruses have been known to survive for long periods in the environment, especially when temperatures are low such as highly pathogenic H5N1 virus can survive in bird feces for more than a month at low temperature. The H5N1 subtype of highly pathogenic avian virus (HPAIV) initially identified during 1996 in China, infected 18 humans with 6 deaths during 1997 in Hong Kong. This virus was highly pathogenic in chickens and humans and posed a crucial threat to public health. In addition, it has been known that H5N1 virus caused more than 60% human mortality, and as of April 2016, H5N1 virus caused of 449 deaths and more than 850 cases-confirmed human infections. Direct or indirect contact with diseased poultry is the primary route of HPAIV infections in humans. Despite of efforts which have been done to prevent of HPAIV spread by whether vaccination or culling of infected birds, several H5 influenza subtypes have already been prevalent in Asia, Europe, and Africa. Therefore, the prevention and rapid detection of H5Nx, especially for highly pathogenic

* Corresponding author.
E-mail address: mbgu@korea.ac.kr (M.B. Gu).

http://dx.doi.org/10.1016/j.bios.2016.06.064
0956-5663/

viruses H5N1, are required to control the outbreak of AI H5Nx.

The aptamers are selected from randomized nucleic acid libraries which has diversity of $10^{12} \sim 10^{14}$ and typical short fragment of single-stranded DNA, RNA or peptide via rounds of affinity capture and amplification in SELEX process (systematic evolution of ligands by exponential enrichment) (Ellington and Szostak, 1990; Tuerk and Gold, 1990). Upon the needs of capturing molecules, hundreds of aptamers were developed to various types of target such as antibiotics, amino acids, toxins, and small molecules or relatively bigger molecules including peptides, proteins, cells, and viruses (Ikebukuro et al., 2005; Lee et al., 2011; Niazi et al., 2008; Nitsche et al., 2007; Adler et al., 2008). Aptamers display a high affinity and specificity to their target molecules, which can be acquired through selection strategies, with impressive dissociation constants (Kd) ranging from picomolar to nanomolar levels between aptamer and its target. Compare to conventional capturing probe, namely antibody, the main advantage of aptamers is their generation using in vitro selection process, whereas the production of antibodies uses biological systems (Song et al., 2012). By isolation of aptamers in vitro condition, various aptamers can be produced to variety of targets without any roadblock of immunogenicity or toxicity. Aptamers are in general thought to be more stable than antibodies, thereby having a longer shelf life. Aptamers are also more sustainable at high temperatures such that they can be regenerated easily after denaturation. Also, chemical modifications or labeling on aptamers are easier and their binding property is not affected by these labeling or modification step. Overall, compared with traditional ligands including antibodies, peptides, and small molecules, the aptamers exhibit advantages such as low cost, low immunogenicity and toxicity, small size to enable solid tumor penetration, and high affinity to bind to the target. Therefore, the aptamers could be the ideal candidates to use in therapeutic, analytical, medical diagnosis, and biosensor applications (Herr et al., 2006; Wang et al., 2011; Yu et al., 2011).

There are a few research papers that have reported the selection of avian influenza virus aptamers for the detection and inhibition of avian influenza viruses. Some research groups have been used HA proteins or peptides, such as purified influenza B virus HA proteins, HA proteins of H5 and H9 in order to select DNA or RNA aptamers (Cheng et al., 2008; Suenaga et al., 2014; Choi et al., 2011; Jeon et al., 2004; Gopinath et al., 2005, 2006b). Interestingly, whole influenza H3N2 virus has been used for RNA aptamer selection to obtain HA-specific RNA aptamer (Gopinath et al., 2006a). Very recently, Wang et al. (2013) reported the selection of influenza H5N1 aptamer from purified HA and whole virus, and then the specific aptamer was applied to develop biosensor for detection AI virus (Wang and Li, 2013). So far, there are no report that use various H5Nx whole viruses for aptamer selection and a pair of aptamers for the detection of H5Nx whole viruses.

In this research, we successfully screened out specific aptamers for H5Nx whole viruses by using Multi-GO-SELEX protocol (Nguyen et al., 2014). Among selected aptamers, a pair of aptamers was obtained and applied to SPR chip for aptamer-based sandwich type detection of the whole virus successfully.

2. Material and methods

2.1. Screening specific aptamer of avian influenza virus (AI) H5 using Multi GO-SELEX

2.1.1. General H5Nx SELEX

To prepare the denatured ssDNA, the 2 μl of 100 μM of 66mer ssDNA's random library is added into 98 μl of 1x binding buffer (BB) and the mixture is heated for 15 min at 95 °C and then slowly cooling down for 5 min on ice. After the 200 μl of 10^6 EID50/ml of counter targets (in BB) and the denatured ssDNA library are gently mixed, the mixture is incubated 30 min at RT by rotating. Then, the 100 μl of GO solution (5 mg/ml), 2 × BB (100 μl), 1 × BB (500 μl) are added in the tube and it is incubated for 2 h, RT, rotator. (Total volume 1 ml, GO 0.5 mg/ml). After that, the mixture is centrifuged at 14,680 rpm for 10 min and then the 800 μl of supernatant is removed. The ssDNA binding to GO is washed 2 times with 1xBB. The 200 μl of 10^6 EID50/ml of three main targets: H5N1, H5N2, H5N3 whole viruses and 1 × BB 700 μl are added in to the reaction tube and gently mixed, then the mixture is incubated for 2 h at RT by rotator. The reaction solution proceeds to centrifuge at 14,680 rpm for 10 min. After supernatant are collected (2 separate tube, 400 μl), the centrifugation process is repeated to remove remaining GO (2 ×). Finally, ethanol precipitation process is conducted by adding Glycogen 3 μl (5 mg/ml), NaOAc 100 μl (3 M), and Isopropanol (same volume as solution), then the solution is incubated for 2 h at −20 °C refrigerator.

2.1.2. Negative SELEX

The 20 μl (2000 ng of ssDNAs) from the 5th round sample in the H5Nx whole virus-based SELEX is added into 80 μl of 1 × binding buffer (BB) and the mixture is heated for 15 min at 95 °C and then slowly cooling down for 5 min on ice. The 500 μl of 10^6 EID50/ml of counter targets (H1N2, H2N1, H3N8, H4N6, H6, H7N8, H9N2, H10N4, H11, H12N5), others viruses (IBV, NDV), Mock allantoic fluid and feces solution (in 1 × BB) are gently mixed with 100 μl of the denatured ssDNAs of the 5th round sample and 500 μl of 2 × Binding buffer, and then the mixture was incubated for 30 min at RT in the rotating rocker. Then, the 100 μl of GO solution (5 mg/ml), 2 × BB (100 μl), 1 × BB (500 μl) are added in the tube, and it is incubated for 2 h at the room temperature in the rotator (total volume 1 ml, GO 0.5 mg/ml). After that, the mixture is centrifuged at 14,680 rpm for 10 min, and then the 800 μl of supernatant is removed. The ssDNA bound to GO was washed 2 times with 1 × BB. The 200 μl of 10^6 EID50/ml of three main target viruses, H5N1, H5N2, H5N3, and 1 × BB 700 μl are added into the reaction tube, and gently mixed, then the mixture was incubated for 2 h at RT in the rotator rocker. Further steps are followed for the general H5Nx SELEX protocol mentioned above.

2.2. Characterization of aptamer candidates using SPR

The binding affinity and the specificity of aptamers were analyzed and characterized using SPR method. The aptamers were immobilized on SPR gold chip using EDC/NHS as following previous studies (Lee, et al., 2008; Liu, et al., 2013; Ahmad Raston and Gu, 2015). Briefly, the surface of SPR was cleaned using ethanol (x3times) and distillation water (× 3 times). Then, the cleaned chip was immersed into the ethanol solution (100%) containing of 50 mM DTP for 14–18 h (overnight) at RT. Then, carboxyl functional groups on chip surface were activated with 200 mM EDC and 50 mM NHS for 30 min. Subsequently, chip was incubated with 100 μg/ml (1.9 μM) of streptavidin for 90 min on ice. The unreacted functional groups were blocked by addition of 50 mM ethanolamine solution for 30 min. Then 5′-T_{10}-biotin labeled aptamers were incubated (1 μM) for 60 min at room temperature. Finally, chip was blocked with 50 μg/ml BSA solution for 30 min and washed with DW. By using this aptamer modified gold chip, SPR (Eco Chemie, Netherlands) analysis was performed after injection of 50 μl of each main target (H5N1, H5N8, and H5N2) and mixed counter targets (H1, H2, H3, H4, H6, H7, H9, H10, H11, H12) as well. The binding reaction was performed for 30 min with a 5 min dissociation time at room temperature. To analyze the dose dependent and Kd value, 5 aptamers with high specific to AI H5 were selected from out of 18 aptamer. The dissociation constant

was determined with the nonlinear regression analysis.

2.3. Synthesis of gold-nanoparticles (AuNPs)

The AuNPs were synthesized by using citrate reduction of $HAuCl_4$ protocol as reported previously (Liu and Lu, 2006). The size and monodispersed production of the AuNPs were confirmed by transmission electron microscopy (Tecnai 20) and UV/Vis spectrophotometry (Ultraspec 6300 pro, Amersham Biosciences, Piscataway, NJ, USA). The synthesized AuNPs were about 13 nm in diameter, spherically shaped, with a deep red color. The concentration of these unmodified AuNPs was estimated by the Beer-Lambert law using an extinction coefficient of $2.43 \times 10^8\ M^{-1}\ cm^{-1}$ at 520 nm.

2.4. Circular Dichroism studies (CD)

The conformational changes of the aptamer upon binding of virus targets were investigated using CD measurements. The experiments were carried out using solutions of 1 μM aptamer and 10^6 EID50/ml of H5N1 virus within a quartz cuvette with 1 cm path length in an optical chamber.

2.5. Confocal microscopy analysis

Immobilization of the biotinylated probes on the surface of the streptavidin coated QDs and MBs was achieved using the avidin–biotin interaction, following previously reported protocol (Kim et al., 2007). The magnetic beads (MB) coated with streptavidin were functionalized with 5′-biotinylated IF10 using the protocol suggested by manufacturer. Before immobilization, 50 μl of the streptavidin modified magnetic beads (10 mg/ml, approx. $7–12 \times 10^9$ beads) were washed two times with 100 μl of 2 × Binding & Washing (B&W) buffer (10 mM Tris–HCl, pH 7.5, 1 mM EDTA, 2.0 M NaCl) to remove any preservatives and then re-suspended in 100 μl of 2 × B&W buffer. Next, 100 μl of the MB-probes (10 μM), in distilled water, were mixed with the washed MBs suspension and incubated for 10 min at room temperature with gentle agitation. The magnetic beads, now coated with MB-probes, were separated from the weakly bound MB-probes and washed three times with 1 × B&W buffer using a magnet.

2.6. The preparation of AuNP-secondary aptamer conjugation

The selected reporter aptamer was immobilized on the surface of gold nanoparticles (AuNP) according to previously reported procedure with slight modifications. Briefly, mono-dispersed AuNPs were synthesized and stabilized with citrate. A transmission electron microscopy (TEM, Tecnai 20) confirmed the average size of AuNPs as 13 nm. To conjugate thiolated reporter aptamer to AuNPs, 2 ml of prepared AuNPs (15.5 nM) were transferred to NaOH-treated vial and then 10 μl of thiolated reporter aptamer (50 μM) which had been already stabilized with TCEP was added. The 10 μl of 50 μM 2nd aptamer were immobilized on AuNPs using salt aggregation method to obtain the aptamer conjugated AuNPs. The free-thiolated aptamer was removed and then collected by centrifugation. The ethanol precipitation process is conducted to collecting the free-thiolated aptamer. The free-thiolated aptamer were not found and the aggregates were not observed in experimental procedures. Therefore, the ratio of Aptamer: AuNP is estimated around 16 per a gold particle. This number was obtained by following steps: First, we mixed the known amount of the aptamers with the known amount of AuNPs. After the unbound aptamers were estimated by using the nanodrop after separation, the ratio 16:1 (aptamer: AuNPs) was obtained by the number of aptamers bound divided by the number of AuNPs added. The mixture was stored with gentle stirring at room temperature for 16 h. After making covalent bonding between sulfur and gold, the reporter aptamer-modified AuNPs were obtained. Free-thiolated aptamer was removed by centrifugation at 14,000 rpm for 25 min and the precipitates were washed with 5 mM Tris–HCl (pH 7.4) two times. The MCH (6-mercapto-1-hexanol) was used for efficient blocking of unoccupied region on the surface of AuNPs. MCH with final concentration of 10 μM was added to aptamer-modified AuNPs conjugates and incubated at room temperature for 30 min and stored at 4 °C at 8 h. After MCH blocking, the conjugates were washed with 5 mM Tris–HCl (pH 7.4) two times. No aggregates were observed in experimental procedures.

3. Results and discussion

3.1. Successful screening of aptamers binding to AI H5Nx viruses

The specific aptamers binding to H5Nx viruses were screened from the random DNA library by using Multi-GO SELEX. In the course of GO-SELEX, from 1st to 5th round, firstly, the denatured ssDNAs were incubated with GO solution to adsorb onto GO surface via π-π stacking interaction. Then after the supernatant was discarded, the ssDNAs may retain in solution. When the mixture of H5Nx whole viruses were added into solution, the specific DNAs bounded to H5Nx viruses detached out from GO surface, and returned back to the solution phase through target-induced mechanism. The Fig. 1 showed that the recovery of bound ssDNAs/total ssDNAs was increased from 1.6% to 68.2% in the course of GO-SELEX. Moreover, the fact that the yield after the 5th round was 68% which is similar yield at the 4th round (64.9%), indicated the saturated state of bounded ssDNAs in the progress of SELEX. After the 5th round of selection, subsequently, the negative SELEX was performed to eliminate the ssDNAs non-specifically binding to the counter-target viruses. The counter-target virus samples were composed of HA virus Negative Selection (H1, H2, H3, H4, H6, H7, H9, H10, H11, H12), NA virus Negative Selection (N1, N8 and N2), other counter virus such as Infectious bronchitis virus (IBV), Newcastle disease virus (NDV), and wide bird's feces buffer solution as an assay buffer in field. The recovery after this negative SELEX step was dropped down to 28%, probably due to some strong competitive binding and non-specific binding with the counter virus samples. Thereafter, the post-SELEX was carried out to increase the recovery of the enriched ssDNAs from the random pool, and after the 7th round of Multi-GO-SELEX, the enriched ssDNAs were cloned and sequenced. As a result, total 18 aptamer candidate sequences were finally collected and their features, including their Gibb's free energy and secondary structures, were elucidated (See Table S1 and Fig. S3 in SI). Furthermore, total 18 sequences of aptamer candidates were individually characterized using SPR assay as can be seen in Fig. 2. Among total 18 candidate sequences, 13 sequences of aptamer candidates showed the affinity binding to some of H5Nx whole viruses. Interestingly, the specific bindings of these 13 aptamer candidates could be classified into 3 groups, according to the affinity binding characteristics to 3 highly pathogenic whole virus targets H5N1, H5N2, and H5N8 (IF1, IF4, IF9, IF10, IF12, IF21), to 2 target viruses, H5N1 and H5N2/H5N8 (IF7, IF15, IF19, IF20), or to a target H5N1/H5N8 (IF6, IF22, IF23) (Table S2). The six aptamers (IF1, IF4, IF10, IF12, IF21, and IF22), which showed lower nonspecific binding to the counter viruses, but highly specific binding to H5Nx whole viruses, were chosen out of these 13 aptamers in order to evaluate the binding strength. The binding events of these aptamers to H5N1 virus was also confirmed by Circular Dichroism (CD) analysis. In order to analyze the conformational change of the aptamer and target-induced H5N1 whole virus-bounded forms of the aptamers in

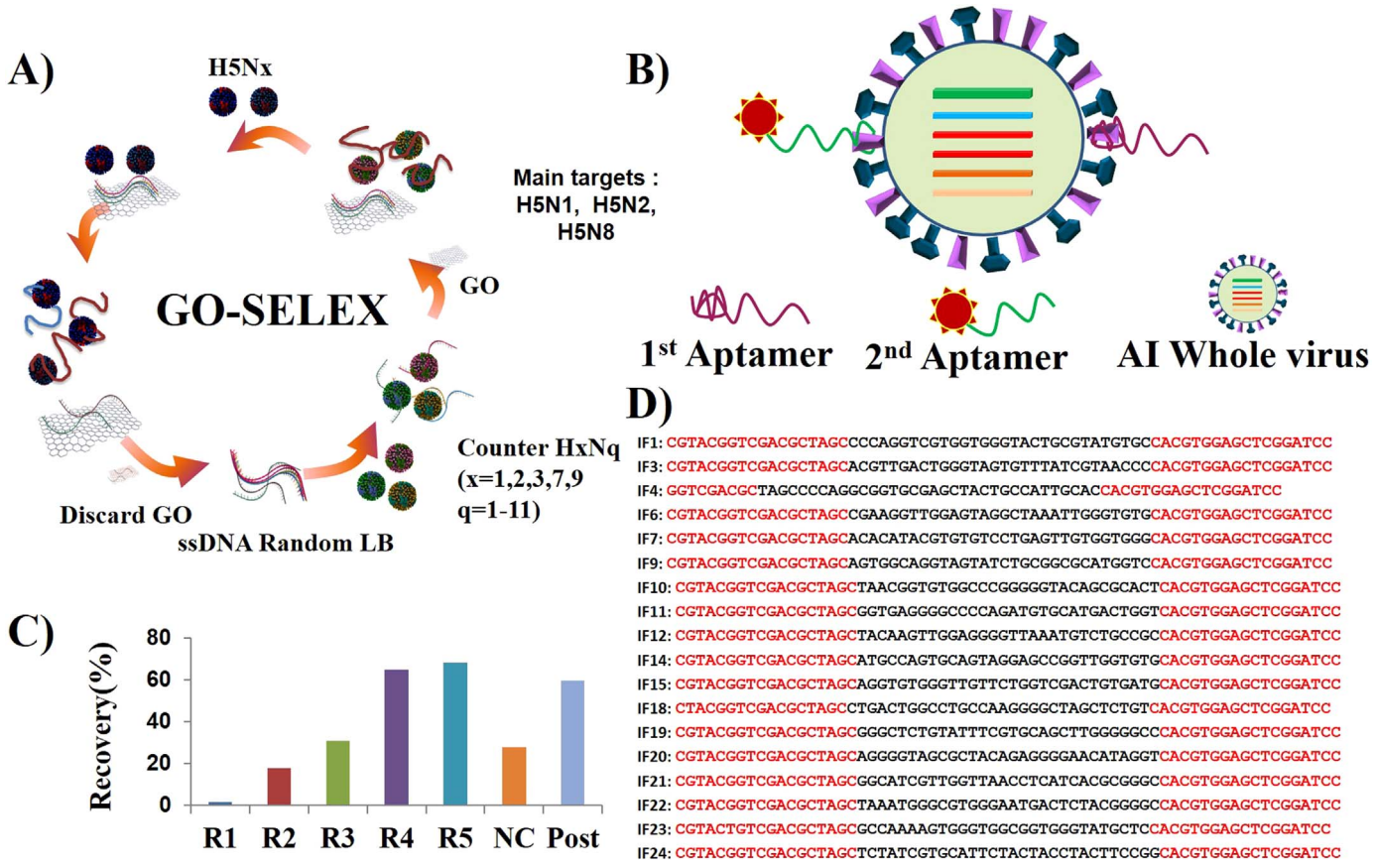

Fig. 1. Screening avian influenza virus specific aptamers using multi-GO-SELEX. A) Schematic illustration of SELEX process of aptamer. B) Schematic illustration on the sandwich-type bindings of a pair of aptamers on the target virus. C) A bar graph showing the percent recovery of target-bounded ssDNAs from 66mer random ssDNA pool library. D) The sequences of aptamer candidates.

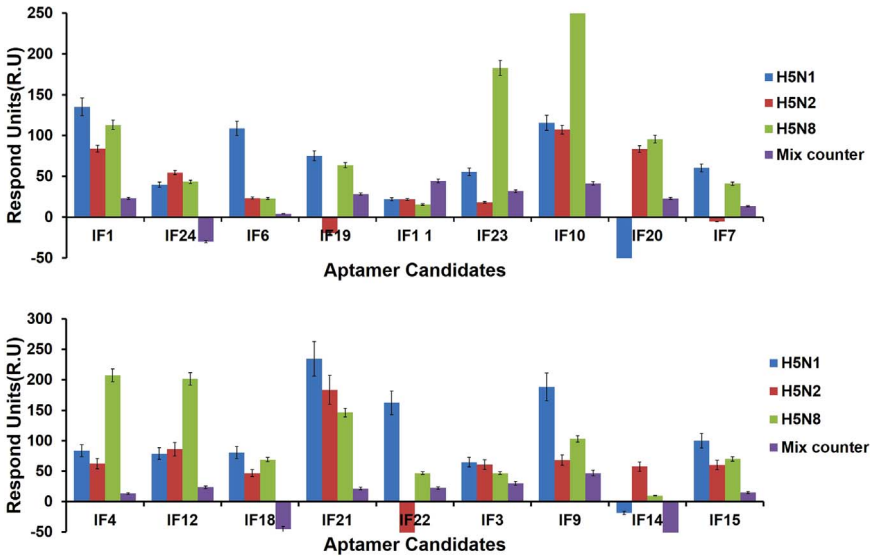

Fig. 2. The specific binding of 18 aptamers. The intensity (RU) of 18 aptamers correspond to H5N1, H5N2, H5N8 whole virus and mixture of counter virus.

solution, the 1.6 ml of 1 μM aptamer solution, 1×10^6 EID50/ml H5N1 virus in buffer solution and the mixture of aptamer and H5N1 virus were simultaneously measured and analyzed by using Circular Dichroism (CD) method. As shown in Fig. 3B, upon the addition of H5N1 virus, IF1, IF4, IF10, IF12, IF21, and IF22 aptamers changed to different peak patterns, compared to their own CD spectra (also see Fig. S6 in SI). The analysis results for each peak changed or shifting were listed in Table S3. In all case of aptamers, the CD spectra are similar to typical B-DNA, which showed trough and positive peaks at 240 and 280 nm, respectively. In the present of H5N1 whole virus, all the peaks/troughs were shifted or were disappeared and new peak/trough were formed, which indicate the conformational changes of aptamer though the recognition binding of the aptamers to whole viruses. It could be used as evidence for the relative binding affinities of the H5N1 whole virus- toward these IF1, IF4, IF10, IF12, IF21, IF22 aptamers.

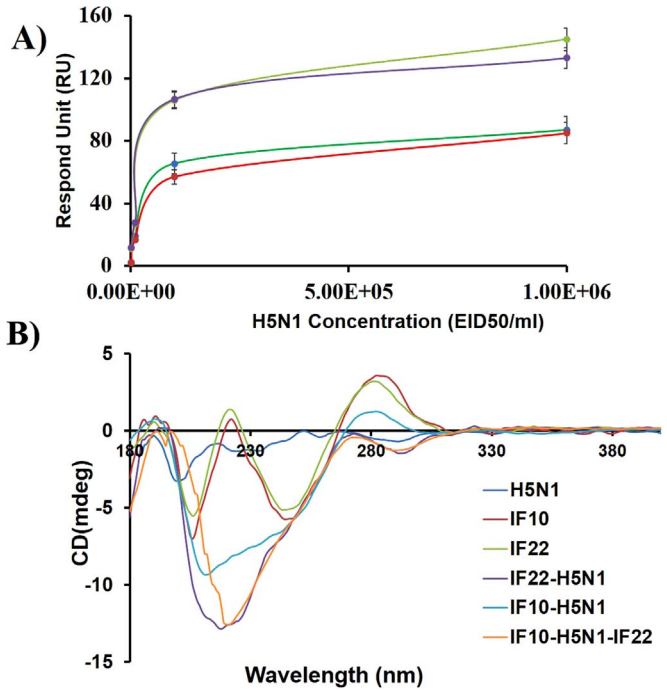

Fig. 3. Analysis of the selected aptamer candidates that shows specificity based on surface plasmon resonance (SPR) analysis. The change in the response unit for various concentrations of H5 viruses was monitored. (A) Dose dependent assay of selected aptamers using SPR assay. B) Circular Dichroism (CD) analysis on the binding of a pair of aptamers to the target virus.

Subsequently, the binding affinities of these aptamers were evaluated with a dose-dependent binding assay and their dissociation constants (Kd values) were calculated to 4.08×10^4, 3×10^4, 7×10^4, and 8×10^4 EID50/ml, for IF1, IF4, IF10, and IF21, respectively (Fig. 3).

3.2. A pair of aptamers for H5N1 Whole virus detection

The binding of six aptamers, IF1, IF4, IF10, IF12, IF21, and IF22 with H5N1 were shown to be concentration dependent in a range from 10^4 to 1×10^6 EID50/ml (Fig. 3A also see Fig. S5 in SI). As shown in Fig. 3A, the angle shift value of SPR chip, on which the selected H5N1 virus aptamers were immobilized, were found to be very small and even minus in some case. So, it was not possible and even unclear to measure the differences in angle shift data of SPR for the concentrations of virus particles below 10^4 EID50/ml. Moreover, the detection range based on SPR analysis was not sufficient for the detection of H5N1 whole virus in real samples. Therefore, possible secondary interactions among three selected aptamers were investigated with an aim of finding a novel aptamer pair and could be applied to a sandwich-type assay. The matrix-wise SPR assays for 6×6 combinations of the selected six aptamers were conducted to screen a pair of aptamers (Fig. 4). In the first step, 6 different chips, on which a specific aptamer as a capture probe (IF1, IF4, IF10, IF12, IF21, and IF22) was immobilized, were incubated with 10^6 EID50/ml of H5N1 whole virus. In second step, the 1 μM of IF1, IF4, IF10, IF12, IF21, and IF22 unmodified aptamers were simultaneously injected on each chip to find the best pair of aptamers when the secondary binding is occurred. However, unfortunately, the increased signal intensities upon the binding of 2nd unmodified aptamer to H5N1 whole virus were very low, compared with the intensity when the H5N1 virus detection occurred in the first step, probably due to the difference of sizes and masses of whole viruses compared to 66mer ssDNA aptamers.

Interestingly, however, in this screening of a pair of aptamers, we found 4 pairs of aptamers, including IF1-IF12, IF4-IF22, IF10-IF12, and IF10-IF22 that have the slightly enhanced intensities around 10RU which may have potential in binding to the different sites of the H5N1 virus.

3.3. Amplification of H5N1 detection using the pair of aptamers by using gold-nanoparticle conjugation

We found that the aptamer IF10 is capable of participating in the secondary binding interaction when the aptamer IF22 was immobilized on as a capturing probe, indicating that two aptamers' binding sites are different and the combination is in harmony. Regarding the reverse combination, no binding was observed, probably due to the affinity differences and other subtle parameters, such as different ranges of optimum concentrations of both aptamers affecting on the sandwich binding.

steps within these limited experiments aimed to confirm aptamer-based sandwich bindings with fixed concentration (1 μM). The pair of aptamers has a capability to easy and broad modification of capturing and reporting aptamers in order to enhance the detection of target in sensing platform. Since the sandwich-type SPR-based assay using bare IF22 reporting aptamer showed only a small increment in the SPR signal, we, therefore, performed a signal enhancement approach by conjugating AuNPs to the IF22 reporting aptamer (Fig. 5A). As can be seen in Fig. 5C, the sandwich system using the aptamer conjugated with AuNPs showed highly enhanced response unit on SPR sensor platform, compared to the use of single aptamer or 2nd aptamer without modification. The signal enhancement assisted by aptamers-conjugated with AuNPs in SPR platforms are shown in Fig. 5C. The angle shift with the aptamers conjugated with AuNPs was considerably increased within the range from 1×10^3 EID50/ml to 1×10^5 EID50/ml, which is more than 50 times enhanced than a single-aptamer based SPR assay or 2nd aptamer without AuNP conjugation, respectively.

The hybridization prediction on the pairing of aptamers, such as IF10-IF22 and IF4- IF22 were determined by using IDT analyzer (https://sg.idtdna.com/calc/analyzer). It is well-known that two different DNAs could be hybridized each other only in high salt condition, such as $4 \times$ SSC buffer, when they have more than 15-mer matching bases for pairing. However, as shown in Fig. S9, the number of matching bases between two different sequence were 7 base pairs and 8 base pairs, corresponding to the pairs of IF10-IF22 and IF4-IF22, respectively. Moreover, in the SPR assay used in this study, the binding buffer (low salt) was used, which won't allow the DNA-DNA hybridization occurred. So, if the false-positive bivalencies exist in this aptamer-based sandwich-type SPR assay, the intensity of SPR signal will be independent on the virus concentration. However, it has not been seen in this study. In addition, since the pair of IF4-IF22 has 8 base-pairing, compared to the pair of IF10-IF22 (known to have 7 base pairs), the response unit of IF4- IF22 pair was 5 times lower than the response unit of IF10-IF22 pair, which indicates that the base pairing between the aptamer pairs were not occurred at all.

The binding of this pair of aptamer combination to H5N1 virus was also confirmed by circular Dichroism (CD) analysis (Fig. 3B). These evidences also supported that this pair of aptamers has a significantly different secondary structure, showing that these two aptamers naturally bind to H5N1 whole virus at the different site. In the same sandwich format like SPR-based assay, we further visualized this dual binding event on H5N1 whole virus by using quantum dot labeled-IF22 reporter aptamer (see Fig. S7 in SI). The biotin labeled IF10 aptamer was used as primary aptamer conjugated on streptavidin coated magnetic bead and biotin labeled IF22 secondary aptamer was then conjugated on streptavidin coated quantum dot. From the confocal laser scanning microscopy

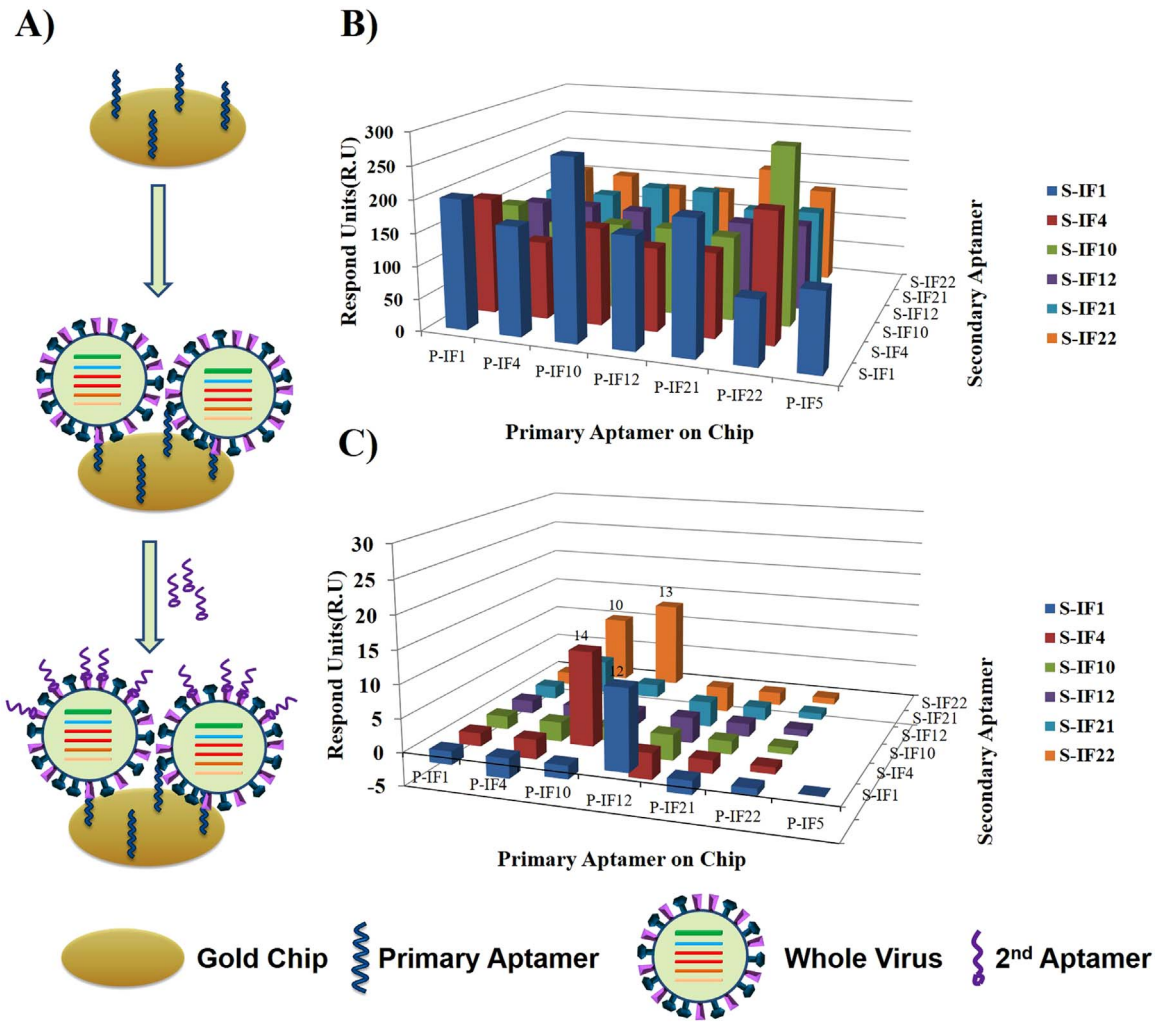

Fig. 4. The dual aptamer finding using SPR. A) The schematic of detection mechanism of aptamer-based sandwich assay. B) The graph present the intensity values of different primary aptamer SPR chip when were injected H5N1 whole virus. C) The intensity values of secondary binding of unmodified aptamer.

(CLSM) analysis, the fluorescent image could be seen only with the presence of H5N1 virus together with the aptamer dual combination. From the plotted SPR response unit in the inset Fig. 6, detection limit was calculated by using blank sample (buffer)+3 standard deviations (SDs) for single and dual aptamer-based systems which were found to be 10,000 EID50/ml and 200 EID50/ml H5N1 whole virus, respectively. Thus, the sensitivity was improved for about 50-fold increased for H5N1 whole virus detection. In addition, the detectable of H5N1 whole virus in this study was 10^3 EID50/ml and the dynamic range of detection was 10^3–10^5 EID50/ml H5N1 whole virus (Fig. 6).

Even though one of the previously published paper (Dovas et al., 2010) reported the detection of virus with a low LOD, this study was based on the molecular diagnosis method which needs the breakage of the viruses and RT-PCR, along with other separation methods, and so this method was completely different from our whole virus based detection without the breakage of the viruses. In addition, the detection sensitivity of ELISA, Dot ELISA or AC-ELISA methods reported in the previously published papers (He et al., 2013; Shim et al., 2015; He et al., 2007, 2010) have been shown that the sensitivity was in the range $10^{1.8}$ to 10^5 EID50/ml (or TCID50/ml), which was comparable with our aptamer-based sandwich-type method. Therefore, this sandwich-type SPR biosensor using a pair of aptamers has great potential to be applied in real field applications.

4. Conclusion

In conclusion, the pair of aptamer IF10-IF22 was successfully found for H5N1 whole virus with high affinity and specificity within the 7th round of SELEX using Multi-GO-SELEX method. This pair of aptamers was successfully applied for detection of H5N1 whole virus by using aptamer conjugated AuNP based sandwich-type SPR method. By applying the selected aptamer pair, highly sensitive detection of 1000 EID50/ml of H5N1 whole virus could be detected. The detection limit of the sandwich-type SPR-based biosensor were found to be 200 EID50/ml whole virus. This dual aptamer-based can be applied to variable sandwich format biosensors.

Acknowledgment

This research was supported by the National Research Foundation of Korea (NRF) grant funded by the Korea Government (MSIP) (No. 2016R1E1A2020541 and No. 2016R1A2B3011422), the Basic Core Technology Development Program for the Oceans and the Polar Regions of the National Research Foundation (NRF) funded by the Ministry of Science, ICT & Future Planning (2015M1A5A1037055) and the KIST Institutional Program (Project No. 2E00000-00-000). The Dr. V. T Nguyen's salary was financially

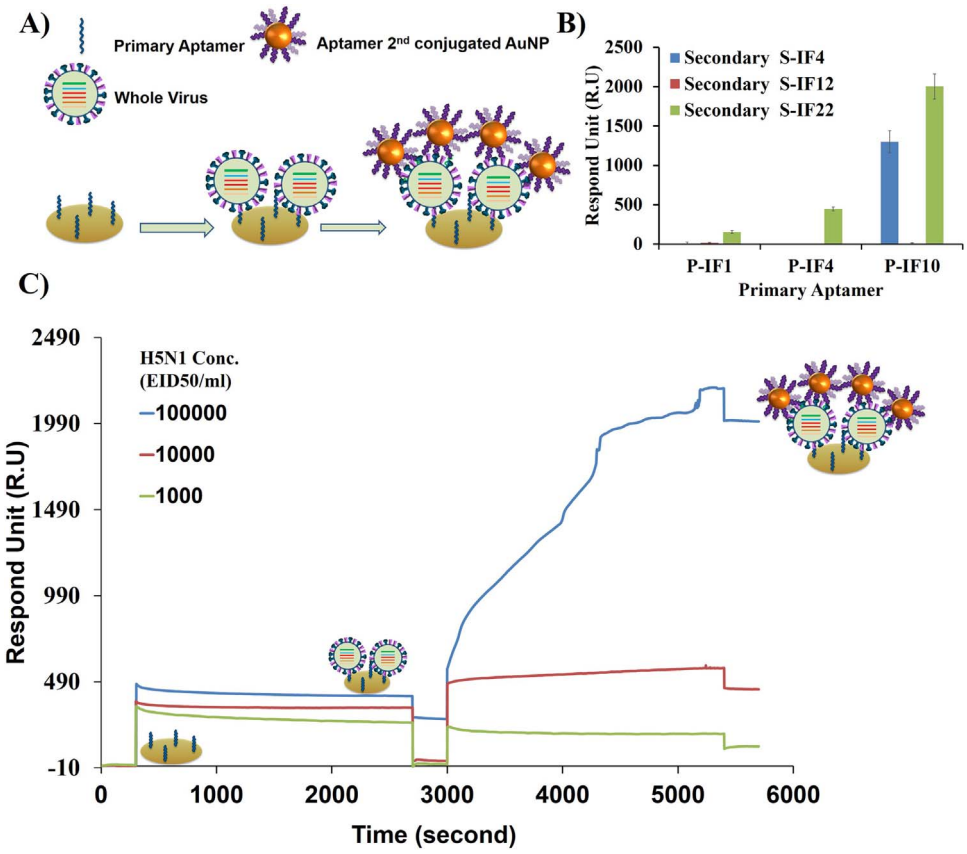

Fig. 5. Dual aptamer using the combination of SPR assay and secondary aptamer conjugated-AuNP. A) The scheme is depicted the principal of SPR assay using secondary aptamer conjugated-AuNP; B) The pair of aptamers IF1-IF12, IF4-IF22, IF10-IF12, and IF10-IF22 were re-checked using aptamer conjugated-AuNP; C) The Dose-dependent binding assays of the pair of aptamer IF10-IF22 using SPR-AuNP.

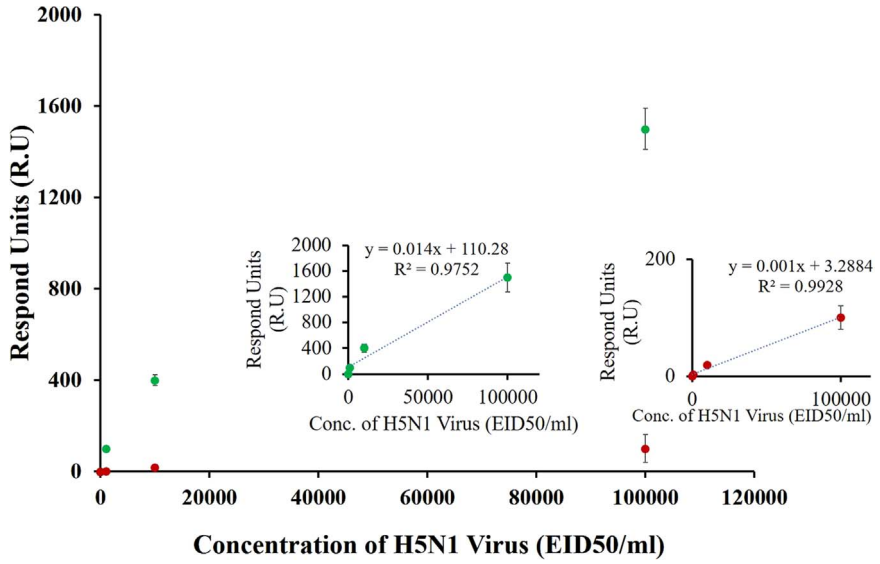

Fig. 6. The comparison of Dose-dependent binding assays by using single aptamer (red line) and dual aptamer-based (green line) for H5N1 whole virus detection measured by SPR-based analysis. The inset figures showed enlarged spectrum analysis of linear range concentration for single and dual aptamer-based from 0 to 10^5 EID50/ml. (For interpretation of the references to color in this figure legend, the reader is referred to the web version of this article.)

supported by Korea University Grant.

Appendix A. Supplementary material

Supplementary data associated with this article can be found in the online version at http://dx.doi.org/10.1016/j.bios.2016.06.064.

References

Adler, A., Forster, N., Homann, M., Goringer, H.U., 2008. Comb. Chem. High. Throughput Screen 11, 16–23.
Ahmad Raston, N.H., Gu, M.B., 2015. Biosens. Bioelectron. 70, 261–267.
Alexander, D.J., 2007. Avian Dis. 51, 161.
Cheng, C., Dong, J., Yao, L., Chen, A., Jia, R., Huan, L., 2008. Biochem. Biophys. Res. Commun. 366, 670–674.

Choi, S.K., Lee, C., Lee, K.S., Choe, S.Y., Mo, I.P., Seong, R.H., 2011. Mol. Cells 32, 527–533.
Dovas, C.I., Papanastassopoulou, M., Georgiadis, M.P., Chatzinasiou, E., Maliogka, V. I., Georgiades, G.K., 2010. Appl. Environ. Microbiol. 76, 2165–2174.
Ellington, A.D., Szostak, J.W., 1990. Nature 346, 818–822.
Gopinath, S.C., Kawasaki, K., Kumar, P.K., 2005. Nucleic Acids Symp. Ser. 49, 85–86.
Gopinath, S.C., Misono, T.S., Kawasaki, K., Mizuno, T., Imai, M., Odagiri, T., 2006a. J. Gen. Virol. 87, 479–487.
Gopinath, S.C., Sakamaki, Y., Kawasaki, K., Kumar, P.K., 2006b. J. Biochem. 139, 837–846.
He, F., Prabakaran, M., Tan, Y., Indira, K., Kumar, S.R., Kwang, J., 2013. BMC Microbiol. 13, 219–228.
He, F., Soejoedono, R.D., Murtini, S., Goutama, M., Kwang, J., 2010. BMC Microbiol. 10, 330.
He, Q., Velumani, S., Du, Q., Lim, C.W., Ng, F.K., Donis, R., Kwang, J., 2007. Clin. Vaccin. Immunol. 14, 617–623.
Herr, J.K., Smith, J.E., Medley, C.D., Shangguan, D., Tan, W., 2006. Anal. Chem. 78, 2918–2924.
Ikebukuro, K., Kiyohara, C., Sode, K., 2005. Biosens. Bioelectron. 20, 2168–2172.
Jeon, S.H., Kayhan, B., Ben-Yedidia, T., Arnon, R., 2004. J. Biol. Chem. 279, 48410–48419.
Kim, Y.S., Kim, B.C., Lee, J.H., Kim, J., Gu, M.B., 2007. Biotechnol. Bioprocess Eng. 11 (5), 449–454.
Lee, J., Jo, M., Kim, T.H., Ahn, J.Y., Lee, D.K., Kim, S., Hong, S., 2011. Lab Chip 11, 52–56.
Lee, S.J., Youn, B.S., Park, J.W., Niazi, J.H., Kim, Y.S., Gu, M.B., 2008. Anal. Chem. 80, 2867–2873.
Li, K.S., et al., 2004. Nature 430, 209–213.
Liu, J.W., Lu, Y., 2006. Angew. Chem. Int. Ed. 45, 90–94.
Liu, L., Deng, D.H., Xing, Y., Li, S.J., Yuan, B.Q., Chen, J., Xia, N., 2013. Electrochim. Acta 89, 616–622.
Nguyen, V.T., Kwon, Y.S., Kim, J.H., Gu, M.B., 2014. Chem. Commun. 139, 4696–4701.
Niazi, J.H., Lee, S.J., Gu, M.B., 2008. Bioorgan. Med. Chem. 16, 7245–7253.
Nitsche, A., Kurth, A., Dunkhorst, A., Panke, O., Sielaff, H., Junge, W., Muth, D., Scheller, F., Stocklein, W., Dahmen, C., Pauli, G., Kage, A., 2007. BMC Biotech. 7, 48.
Shim, D.H., Kim, J.K., Hong, M., Na, W., Park, Y.A., Park, S.J., Song, D., Lee, J.M., Kim, H. K., 2015. J. Virol. Methods., 215–216 9-12.
Song, K.M., Lee, S., Ban, C., 2012. Sensors 12 (1), 612–631.
Suenaga, E., Kumar, P.K., 2014. Acta Biomater. 10, 1314–1323.
Tuerk, C., Gold, L., 1990. Science 249, 505–510.
Wang, J., Zhu, Z., Munir, A., Zhou, H.S., 2011. Talanta 84, 783–788.
Wang, R., Li, Y., 2013b. Biosens. Bioelectron. 42, 148–155.
Wang, R., Zhao, J., Jiang, T., Kwon, Y.M., Lu, H., Jiao, P., Liao, M., Li, Y., 2013a. J. Virol. Methods 189, 362–369.
Yu, C., Hu, Y., Duan, J., Yuan, W., Wang, C., Xu, H., Yang, X.D., 2011. PLoS One 6, e24077.